Science of the Total Environment 619–620 (2018) 1375–1384

Contents lists available at ScienceDirect

Science of the Total Environment

journal homepage: www.elsevier.com/locate/scitotenv

Characterization of engineered nanoparticles in commercially available spray disinfectant products advertised to contain colloidal silver

Kim R. Rogers [a,*], Jana Navratilova [a], Aleksandr Stefaniak [c], Lauren Bowers [c], Alycia K. Knepp [c], Souhail R. Al-Abed [b], Phillip Potter [b], Alireza Gitipour [b], Islam Radwan [b], Clay Nelson [a], Karen D. Bradham [a]

[a] U.S. Environmental Protection Agency, RTP, NC, United States
[b] U.S. Environmental Protection Agency, Cincinnati, OH, United States
[c] National Institute for Occupational Safety and Health, Morgantown, WV, United States

HIGHLIGHTS

- Silver nanoparticles were characterized in products advertised to contain colloidal silver.
- Products showed a high degree of variability for claimed vs. measured total silver.
- Products showed variations in percentages of particulate vs. soluble silver.
- Two size populations were observed; smaller (<5 nm) and larger particles 20–40 nm.
- Plasmon resonance absorbance signatures were only observed in 4 of the suspensions.

GRAPHICAL ABSTRACT

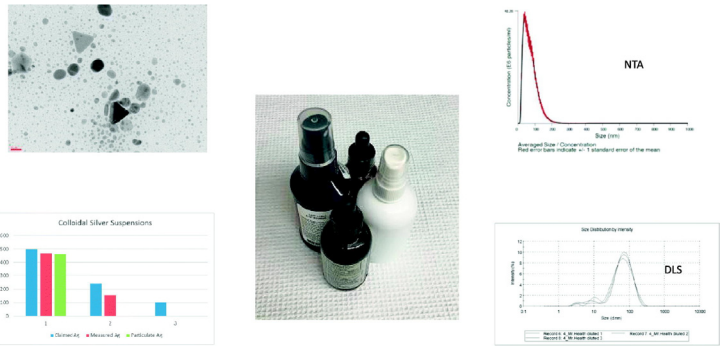

ARTICLE INFO

Article history:
Received 13 September 2017
Received in revised form 16 November 2017
Accepted 17 November 2017
Available online xxxx

Editor: D. Barcelo

Keywords:
Colloidal
Silver
Nanoparticle
Spray disinfectant
Dietary supplement
Human exposure

ABSTRACT

Given the potential for human exposure to silver nanoparticles from spray disinfectants and dietary supplements, we characterized the silver-containing nanoparticles in 22 commercial products that advertised the use of silver or colloidal silver as the active ingredient. Characterization parameters included: total silver, fractionated silver (particulate and dissolved), primary particle size distribution, hydrodynamic diameter, particle number, and plasmon resonance absorbance. A high degree of variability between claimed and measured values for total silver was observed. Only 7 of the products showed total silver concentrations within 20% of their nominally reported values. In addition, significant variations in the relative percentages of particulate vs. soluble silver were also measured in many of these products reporting to be colloidal. Primary silver particle size distributions by transmission electron microscopy (TEM) showed two populations of particles - smaller particles (<5 nm) and larger particles between 20 and 40 nm. Hydrodynamic diameter measurements using nanoparticle tracking analysis (NTA) correlated well with TEM analysis for the larger particles. Z-average (Z-Avg) values measured using dynamic light scattering (DLS); however, were typically larger than both NTA or TEM particle diameters. Plasmon resonance absorbance signatures (peak absorbance at around 400 nm indicative of metallic silver nanoparticles) were only noted in 4 of the 9 yellow-brown colored suspensions. Although the total silver concentrations were variable among products, ranging from 0.54 mg/L to 960 mg/L, silver containing nanoparticles were identified in all of the product suspensions by TEM.

* Corresponding author.
E-mail address: rogers.kim@epa.gov (K.R. Rogers).

https://doi.org/10.1016/j.scitotenv.2017.11.195
0048-9697/

1. Introduction

Due to their unique characteristics and capabilities, metal-containing nanoparticles are increasingly incorporated into a wide range of consumer products. Data bases that track nanomaterial-containing products, such as the Project on Emerging Nanomaterials (PEN)-Nanotechnology Consumer Inventory Products (CPI) and Nanodatabase, currently contain over 450 silver nanoparticle (AgNP)-enabled consumer products (Vance et al., 2015; Hansen et al., 2016). AgNP-enabled products include fabrics (socks, athletic and mountaineering clothing, and children's clothing), plastics (food containers, child cups and articles that may come into contact with multiple users), personal care products (shampoos, lotions, and toothpaste), spray disinfectants, and dietary supplements (advertised as immune boosters, and anti-infection agents) (Wasukan et al., 2015; Quadros et al., 2013; Tulve et al., 2015). Primarily due to their anti-microbial properties, AgNPs are one of the most significant contributors to the nanoparticle-enabled products and in particular, the personal care products. This is significant because the personal care products area is one of the fastest growing market segments for nanomaterial-enabled products (Reed et al., 2014).

One type of silver-containing health care product that has been marketed and used in various applications for the past century contains what is advertised as colloidal silver (loosely defined as suspensions of silver-containing particles between 1 and 1000 nm in size). The US Food and Drug Administration (FDA), however, has indicated that colloidal silver is not "generally recognized as safe and effective" for treating any disease or condition (www.fda.gov). Nevertheless, due in part to a renewed interest in the anti-microbial properties of nanoscale silver particles (AgNP), liquid spray products that contain combinations of ionic and colloidal silver are currently being marketed for a wide range of health, disinfectant, and antimicrobial applications. Depending on the advertising claims and intended use, colloidal silver products may require registration under the EPA Federal Insecticide, Fungicide, and Rodenticide Act (FIFRA) guidelines. Under FIFRA, EPA regulates all pesticides sold and distributed in the United States (www.epa.gov/pesticide-regulation). EPA's pesticide registration process involves a rigorous and comprehensive scientific assessment of these products resulting in registration decisions.

Although many of the colloidal silver products may contain AgNPs, these products have not typically been captured or tracked in the PEN-CPI or Nanodatabase (Vance et al., 2015; Hansen et al., 2016). For example, of the hundreds of colloidal silver products on the market, only 15 are listed in either database and only 3 of the 22 products selected for the current study have been listed. Given the wide range of potential colloidal silver products that may find market value from claims of antimicrobial activity, the potential exists for direct or indirect human exposure and possible health risks. This is important for aggregate human exposures where the potential exists for multiple applications of the same spray product or the use of multiple AgNP-enabled products by the same individual on a daily basis. This is particularly significant in the case of children that may be directly exposed or indirectly exposed during adult use as well as use by higher vulnerability populations (Tulve et al., 2015; Quadros et al., 2013). Few studies, however, have measured the presence of AgNP in colloidal silver products and within these studies, relatively few products were investigated (Reed et al., 2014, Cascio et al., 2015).

The toxicity of AgNPs, primarily to microorganisms but also in mammalian systems, has been shown to be dependent on characteristics such as size, shape, surface coating and matrix-dependent transformations (Tolaymat et al., 2016; Gitipour et al., 2016). Consequently, in order to determine if AgNP-enabled products might result in significant risks to human health or the environment, it is critical to understand the characteristics of these products and the nanoparticles they may contain. Potential exposure pathways for these products include inhalation (Silva et al., 2016), gastrointestinal (Shahare et al., 2013; Mwilu et al., 2013) and dermal (Wasukan et al., 2015) and many of these colloidal silver spray products could involve all 3 exposure pathways.

Although the characteristics of pristine AgNPs purchased from commercial vendors or synthesized in the lab, have been widely studied in biological and environmental matrices, the analysis of these particles in consumer product colloidal suspensions offers some unique challenges. Because of the limited labeling and oversight requirements, as well as the wide range of potential applications for colloidal silver products ranging from spray disinfectants to those advertised as immune boosters, it is difficult to determine from product packaging and labeling alone the actual contents of these products. As suggested from website advertisements and vague product labeling, colloidal silver products may contain any number of forms of silver including silver ion, nanoscale silver oxide, silver chloride, silver sulfide, or metallic silver along with stabilizers and additives ranging from "essential oils" to amino acids.

The characterization of physicochemical parameters in selected colloidal silver-enabled products has been recently reported by several research groups (Ramos et al., 2014; Cascio et al., 2015; Reed et al., 2014; Wasukan et al., 2015); however, characterization of a wider collection of representative colloidal silver spray products has not been reported. Because no single method is available to fully characterize AgNPs especially in complex consumer product formulations, strategies using a number of techniques are required (Argentiere et al., 2016; Hagendorfer et al., 2012; Tulve et al., 2015). Methodologies to characterize nanoscale silver have included commonly used techniques such as DLS, transmission electron microscopy-energy dispersive spectroscopy (TEM-EDS), inductively coupled plasma mass spectroscopy (ICP-MS) (Argentiere et al., 2016), and centrifugal liquid sedimentation (CLS) as well as advanced techniques such as asymmetric flow field flow fractionation (AF-4)-ICP-MS and single particle-ICP-MS (Cascio et al., 2015). Our primary goal for this work was to investigate representative selections from the broad range of consumer products advertised to contain colloidal silver to determine the presence of silver-containing nanoparticles. This was accomplished using commonly reported and more widely accessible methods such as ICP- optical emission spectroscopy (OES), centrifugal ultrafiltration (CF), dynamic light scattering (DLS), nanoparticle tracking analysis (NTA), ultraviolet-visible (UV–Vis) spectroscopy and TEM-EDS analysis. We also report size distribution, shape and hydrodynamic properties of the AgNPs in these products to better understand the potential human exposure risks posed by these consumer products.

2. Methods

2.1. Materials

Twenty-two commercially available colloidal silver spray products were purchased from the internet. These products were advertised as health products intended for internal consumption or as surface sanitizers intended for external use. Products were either packaged in pump spray devices or advertised for spray applications. Secondary standard polystyrene beads (100, 50, 40 nm, traceable to National Institute of Standards) were obtained from Thermo Scientific, Fremont, CA. Nanosilver particles (pvp-stabilized) (5, 10, 20, 50, 75 nm) were obtained from Nanocomposix, San Diego, CA. All other chemicals used were of reagent grade.

2.2. Total silver concentration by ICP-OES

For the determination of total silver in the consumer products, 1 mL of the product was acid digested (in triplicate) with 1 mL of concentrated nitric acid (67–70% Optima™, Fisher Scientific, Inc., Pittsburgh, PA) in a hot block (DigiPrep, SCP Science, Quebec, Canada) at 60 °C for 12 h. Prior to ICP-OES analysis, all samples were diluted 10 fold or greater (depending on the initial concentration) using DI water (DI, 18 MΩ

× cm, Millipore, Bedford, MA). The analysis of the digested samples was performed using an iCAP 6500 Duo ICP-OES instrument (Thermo Scientific, Waltham, MA, USA). For quantification of silver, the spectral line at 328.0 nm was used. Scandium (spectral line 361.3 nm) was used as an internal standard. Commercially available certified reference standards (SCP Science) were used for the preparation of calibration standards.

2.3. Centrifugal ultrafiltration

To estimate the dissolved silver fraction in the consumer products, centrifugal ultrafiltration was used in which 5 mL of the product was transferred to a 10 kDa centrifuge filter unit (Amicon Ultra-15, 10 K, Millipore, Bedford, MA) and centrifuged at 5911 $\times g$ for 20 min. After centrifugation, an aliquot of 1 mL of the filtrate was acid digested (in triplicate) and analyzed as described above.

2.4. Dynamic light scattering (DLS)

DLS measurements were performed with a Malvern Zetasizer Nano ZS (Malvern, UK) equipped with a 633 nm He-Ne laser and operating at an angle of 173°. 1 mL of each product was measured in single-use acrylic cuvettes (Sarstedt, Germany). The measurements were performed at a controlled temperature of 25 °C with an automatic attenuation. For each sample, 3 measurements were performed. Throughout all measurements, the instrument count rate was monitored to ensure a consistent count rate that did not exhibit characteristics of contamination from dust (i.e., sharp spikes in count rate), thermal gradients (i.e., widely fluctuating count rate), or aggregation or sedimentation (increasing/decreasing count rates). Though no specific guidance is available on a "good" count rate because other parameters also influence data quality (length of run, number of runs, etc.), for nearly all products the count rates were on the order of 100 to 300 k counts per second. The only exceptions were for Products 6 and 21 for which the count rates were below 50 k counts per second. Polystyrene beads 40, 50, 100 nm (NIST beads; Thermo Scientific, Fremont, California) and pvp-stabilized silver nanoparticles (5, 10, 20, 50, 75 nm, NanoComposix) were used for a quality control. The intensity size distribution, the Z-average diameter (Z-avg), and the polydispersity index (PDI) were obtained from the autocorrelation function using the "general purpose model".

2.5. Nanoparticle tracking analysis (NTA)

NTA measurements of the consumer products were performed with a NanoSight NS500 instrument (NanoSight, UK), equipped with a 640 nm laser. Measurements were performed at 25 °C. All samples were measured for 60 s with manual shutter and gain adjustments. The measurement settings were optimized using 100 nm polystyrene beads. The software used to capture and analyze the data was the NTA 2.3 (NanoSight Ltd.). Each video was analyzed to give a particle size distribution and an estimate of the particle concentration.

2.6. UV–visible spectrophotometry (UV–vis)

The presence of laboratory synthesized or commercial AgNPs in aqueous suspension is often indicated by a light yellow to brown color and absorbance peaks at or around 400 nm due to local surface plasmon resonance (LSPR). UV–visible spectra were collected using a Hewlett Packard single beam instrument (Agilent, Santa Clara, CA) at 25 °C. Concentrated AgNP suspensions were diluted with deionized water which was then passed through a 0.2 μm filter (DI) water to an initial absorbance of about 1.0. Spectra (from 300 to 600 nm) were recorded in the second to minute timeframe.

2.7. Transmission electron microscopy-energy dispersive spectroscopy (TEM-EDS)

TEM-EDS was used to verify the presence of nanoparticles in the consumer products and to measure their size and shape. Two types of grids and two TEM instruments were used. Samples were prepared by depositing a drop of the consumer product onto carbon-coated nickel grids and allowing it to dry in air overnight at room temperature. A JEOL-1200 EX (JEOL Ltd.) operating at 120 kV was used to acquire images at magnifications between 25 kX and 350 kX. The image processing program Image J (NIH) was used to determine the nanoparticle size distributions from TEM micrographs. In separate TEM experiments, AgNPs were applied to amine functionalized silicon dioxide grids (Dune Scientific, Eugene OR) by leaning the chemically modified side of the grid against a sample drop (placed on para-film) for 10 min. The grids were then rinsed by placement in DI water for 15 s and allowed to dry. Micrograph images were obtained using an FEI Titan 80–300 probe aberration corrected scanning TEM with a monochromator operating at 200 kV. A Bruker 4 SDD Energy Dispersive Spectroscopy (EDS) instrument was used to perform elemental mapping. Images were acquired at 300 kV. All images were representative of at least 3 grids. Image J size calculations were conducted using particle counts of 100 to 1000 particles. For the larger particles, size range values were typically determined from observations of between 10 and 20 particles.

2.8. Methods strengths and limitations

Each method used for this study shows inherent strengths and limitations for characterizing AgNPs (Table S-1). Limitations can become somewhat more problematic when investigating these complex mixtures that are often encountered in real-world samples (Steinhäuser and Sayre, 2017). In particular, hydrodynamic diameter measurements by DLS or NTA typically report larger values than for TEM primary sizes particularly for small particles (<20 nm) (Cascio et al., 2014). Differences between primary particle size observed by TEM and hydrodynamic diameter measured using NTA or DLS may be reflective of surface coatings or particle aggregation in suspension. Our observation of commercial AgNPs as well as those of the manufacturer, were consistent with the hydrodynamic measurements being larger than primary particle size measurements by TEM (Table 1). Although NTA can separate particulate populations based on large differences in refractive index; in complex mixtures, this method does not distinguish AgNPs from particles bound to organic aggregates. ICP-OES in combination with centrifugal ultrafiltration can separate particulate and soluble fractions; however, complex matrices can interfere with this process. Protein aggregates and organic micelles tend to clog pores and interfere with the separation process. Although TEM is a fundamental technique often used in nanoparticle characterization, instrument purchase and maintenance is expensive. In addition, sample preparation, dehydration artifacts and image selection can bias results toward expected or novel particles rather than representative analysis.

3. Results & discussion

The colloidal silver products characterized in this study varied widely in both their proposed application, appearance, and formulation. General application areas for these products included dietary supplements, intended for internal consumption and surface sanitizers intended for external use (Table 2). The reported formulation components ranged from colloidal silver in water to addition of "herbs", amino acids, "essential oils", and hydrogen peroxide. These additional organic compounds present in the nano-enabled consumer products may interact with the AgNPs leading to interferences in measuring the hydrodynamic diameter and other parameters. Because of potentially complex product formulations, characterization of AgNPs in consumer products may lead to some

Table 1
Standard polystyrene and commercial AgNP hydrodynamic diameter.

Hydrodynamic diameter							
Particle & source	Nominal size (nm)	TEM nominal Size (nm)	NTA mean (nm)	NTA mode (nm)	DLS_Z-Avg	(PDI)	Nominal Z-Avg (nm)
Polystyrene, NIST	100	100 ± 3	101 ± 0.3	94 ± 0.7	109 ± 0.7	0.03 ± 0.01	nr
Polystyrene, NIST	50	46 ± 2	43 ± 2.3	20 ± 0.9	61 ± 0.6	0.21 ± 0.02	57
Polystyrene, NIST	40	41 ± 4	45 ± 0.5	26 ± 1.7	42 ± 0.2	0.03 ± 0.01	nr
AgNP, NCX	5	4.6 ± 0.6	45 ± 2.1	26 ± 1.6	16 ± 0.49	0.3 ± 0.02	nr
AgNP, NCX	10	9.7 ± 1.8	76 ± 1.2	54 ± 3.3	86 ± 7.5	0.4 ± 0.06	19
AgNP, NCX	20	20.6 ± 3.1	50 ± 0.4	40 ± 0.6	88 ± 2.4	0.4 ± 0.06	41
AgNP, NCX	50	47 ± 4	84 ± 0.4	75 ± 1.1	80 ± 0.7	0.12 ± 0.01	62
AgNP, NCX	75	74.3 ± 3.9	96 ± 1.1	75 ± 0.8	105 ± 0.46	0.04 ± 0.01	98

Silver nanoparticles (AgNP).
Nanoparticle Tracking Analysis (NTA).
National Institute of Standards and Technology (NIST) secondary standard.
NanoComposix (NCX).
nr not reported.
Nominal, TEM nominal and nominal Z-Avg sizes were reported by the manufacturer.

uncertainties in measurements not typically observed for pristine particles. For example, in the case of hydrodynamic diameter measurements using ensemble techniques, such as DLS, protein aggregates or micelles may increase Z-average values assumed to represent AgNPs. These larger particles may also interfere with NTA single particle measurements.

In addition to observable product variations such as color, turbidity, surface tension and odor (due to volatile compounds associated with essential oils), significant variations were also observed in pH, ranging from 2.5 to 10.6. Concentrations of chloride ions were measured by ion chromatography and total elemental sulfur, sodium and potassium (measured using ICP-MS) also showed significant variations among products (Table S-2). The presence of chloride and sulfide ions would be expected to form precipitates with free silver ions in suspension (Sekine et al., 2014).

3.1. Total silver determination

All consumer products tested were advertised to contain some form of silver (colloidal, hydro-sol or ionic) and concentrations were listed on labels for all but three products. Total silver measured by ICP-OES varied significantly among products ranging from 0.54 mg/L to 960 mg/L. Some of the measured concentrations were fairly close to the labeled Ag values while others were either above or below the claimed values (Table 2). For example, products 5, 6, 12, 13, 16, 18, and 22 showed silver contents within 20% of their reported values. The total silver value of 21.5 mg/L for product 16 corresponded closely with the previously reported value of 21.3 mg/L for the same colloidal silver product (Reed et al., 2014). Products 1, 2, and 3, however, yielded only 15, 0.5, and 9.2%, respectively, of their claimed concentrations of silver. Several products that did not list silver concentrations (products 7, 8, 20) showed relatively low total silver (between about 6 and 8 mg/L) as compared to many of the other products (Table 2).

Variability of active ingredients in dietary supplements is not uncommon. Colloidal silver containing products have also been shown to have significant variations between reported and measured silver for both total silver and colloidal silver content (Cascio et al., 2014, 2015). In another study of colloidal silver containing products, total silver concentrations were show to vary over 5 orders of magnitude (Wasukan et al., 2015).

Table 2
Consumer product silver concentration claimed, measured, form (soluble, particulate).

Product	Description	Color	Claimed Ag (mg/L)	Total Ag (mg/L)	Filtrate Ag (mg/L)
1	Colloidal/ionic Ag, dietary supplement	Colorless	120	18.91 ± 0.89	18.61 ± 0.51
2	Colloidal Ag, dietary supplement	Colorless	100	0.54 ± 0.93	bdi
3	Colloidal Ag, dietary supplement	Yellow-brown	15	1.39 ± 0.44	bdi
4	Colloidal Ag, immune support	Dark brown	500	960.82 ± 28.64	4.86 ± 0.03
5	"Silver-sol", ionic Ag, immune support	Colorless	10	9.92 ± 0.94	5.84 ± 0.64
6	Colloidal/ionic Ag, dietary supplement	Dark brown	200	205.04 ± 9.90	2.13 ± 0.04
7	Colloidal Ag, foot spray	Turbid yellow	nr	5.98 ± 1.10	bdi
8	Colloidal Ag, sanitizing spray	Turbid yellow	nr	6.12 ± 0.10	bdi
9	"Silver-hydrosol" Ag, immune support	Colorless	10	12.16 ± 1.47	11.79 ± 0.41
10	Colloidal/ionic Ag, anti-infection	Colorless	240	169.03 ± 3.00	57.50 ± 2.12
11	Colloidal/ionic Ag, anti-infection	Colorless	10	5.22 ± 0.50	4.66 ± 0.01
12	"Silver-sol" Ag, dietary supplement	Colorless	10	9.37 ± 0.67	9.28 ± 0.03
13	Colloidal Ag, throat spray	Orange	30	33.46 ± 0.69	0.02 ± 0.02
14	Colloidal Ag, anti-microbial	Colorless	20	11.78 ± 1.54	6.60 ± 0.14
15	Colloidal Ag, immune support	Colorless	30	53.56 ± 2.40	31.28 ± 0.97
16	Colloidal Ag, dietary supplement	Yellow-brown	20	21.50 ± 3.40	9.99 ± 0.05
17	Colloidal Ag	Colorless	25	28.68 ± 0.32	25.81 ± 0.86
18	Ionic Ag, anti-microbial, immune support	Colorless	10	10.12 ± 0.57	9.84 ± 0.84
19	Ionic Ag, first aid spray	Colorless	20	14.34 ± 1.90	11.48 ± 0.14
20	Colloidal Ag, sanitizing spray, H_2O_2	Yellow	nr	8.72 ± 0.72	0.02 ± 0.01
21	Colloidal Ag, skin spray	Colorless	30	49.10 ± 1.24	31.60 ± 0.32
22	Ionic Ag, dietary supplement	Light yellow	20	19.55 ± 0.10	14.59 ± 0.01

nr not reported.
bdl - below detection limit.

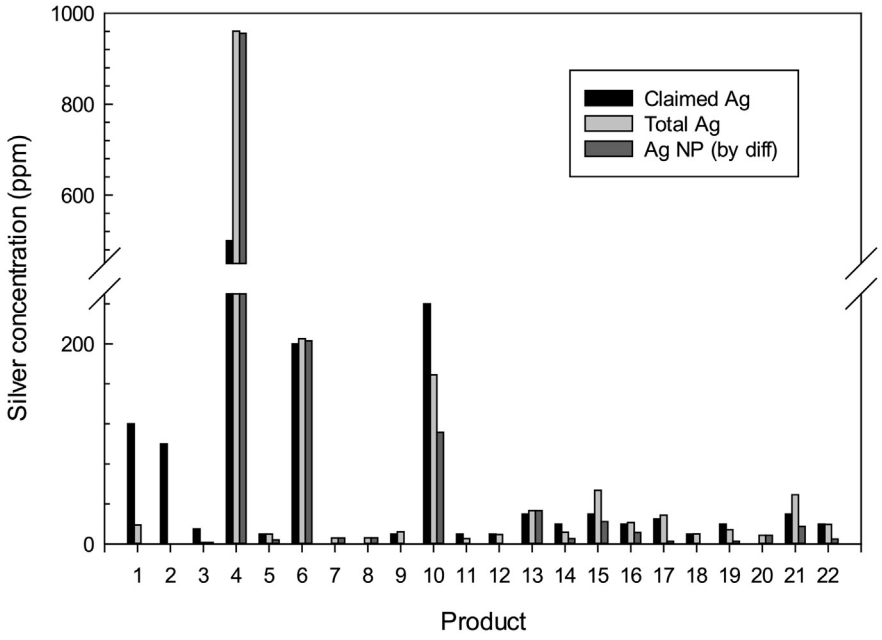

Fig. 1. Total silver determination. Total silver was determined using ICP-OES, claimed silver was reported from product labels and particulate silver was determined as the difference between total silver and silver measured in the filtrate passing through the 10 kDa filter cartridge.

3.2. Particulate vs. soluble silver

Silver concentrations for the 10 kDa filtrates varied significantly among products, indicating that some of the suspensions contained primarily soluble forms of Ag while for others, the silver content was predominantly particulate in nature (Table 2, Fig. 1). For example, products 2, 3, 4, 6, 7, 8, 13 and 20 primarily contained particulate Ag; products 5, 10, 14, 15, 16 and 21 contained both particulate and soluble forms; and for products 1, 9, 11, 12, 17, 18, 19, and 22, the silver was primarily soluble. For four of the products, the amount of Ag in the filtrate was below the method reporting limit of 10 μg/L for ICP-OES.

Ultrafiltration membranes are well described with respect to the separation of globular proteins; however, very small (<5 nm) AgNPs may pose unique challenges for separation of soluble from particulate species. Average pore sizes for 10 kDa molecular weight cut off filters used in centrifugal filtration have been estimated at 3.2 ± 2.3 nm (Van Koetsem et al., 2017). These investigators further indicated that a 10 kDa membrane was suitable for separating 14 nm AgNPs from the ionic Ag fraction. Although our protocol effectively separated commercially available 5 nm AgNP from ionic silver (data not shown), we cannot exclude the possibility that some of the very small (<3 nm) particles identified by TEM (see Table 3) may have passed into the filtrate sample and were counted in the soluble fraction.

3.3. Local surface plasmon resonance

Local surface plasmon resonance (LSPR) was used to identify the presence of metallic AgNPs. Although the use of LSPR has been shown to be a rapid and simple method to identify the presence of metallic AgNP in the size range of 10–50 nm, spectra can be difficult to interpret due to matrix effects (Chinnapongse et al., 2011). The particle size and shape-dependent absorbance peak around 400 nm can be shifted or broadened due to surface interactions among particles or between particles and the suspension matrix (Rogers et al., 2012). The products varied in color from dark brown to yellow-brown to colorless. Four of the products (4, 6, 13, 16), showed absorbance spectra characteristic of LSPR bands for AgNP (Fig. 2). Two of the products were highly concentrated and required serial dilution (1 to 10 in DI water) prior to measurement while for two products absorbance spectra were recorded from the undiluted suspensions. Although silver-containing nanoparticles were observed by TEM in all of the products, five of the nine yellow or brown suspensions did not show LSPR absorbance spectra (products 3, 7, 8, 20, and 22). This result may have been due to the low concentration of metallic silver particles as compared to other silver particle forms (AgCl, Ag_2S, which do not show LSPR absorbance). Each of these products contained a greater mass ratio and some a greater stoichiometric ratio of Cl^- to total Ag (Table S-2). This would suggest that any free Ag^+ would be expected to precipitate, possibly forming AgCl nanoparticles. In addition, the interaction of organic coatings at the particle surface which may include the binding of the AgNPs to

Table 3
Particle size; hydrodynamic diameter, primary particle size.

Hydrodynamic diameter					TEM particle diameter	
Product	NTA Mean (nm)	NTA Mode (nm)	DLS_Z-AVG (nm)	PDI	P-1 (nm)	P-2 (nm)
1	82 ± 1.8	52 ± 2.1	166.9 ± 31.47	0.43	2.3	30–200
2	na	na	284.7 ± 29.53	0.51	nd	200
3	39 ± 2	25 ± 0.4	264.1 ± 17.26	0.45	6.6	nd
4	71 ± 1.4	39 ± 1.3	57.46 ± 0.90	0.46	4.5	20–40
5	96 ± 4.8	66 ± 2	82.99 ± 5.59	0.69	9.1	20–60
6	70 ± 0.7	64 ± 3	55.91 ± 15.69	0.42	3.6	15–40
7	168 ± 23.2	63 ± 13.1	245.5 ± 11.62	0.29	15.5	15–30
8	39 ± 29.7	20 ± 13.4	220.2 ± 5.86	0.34	5.2	15–30
9	105 ± 8.1	64 ± 2.51	68.4 ± 100.2	0.47	10.1	15–100
10	220 ± 28.1	52 ± 6.2	484.4 ± 224.8	0.72	5.1	20
11	72 ± 0.4	64 ± 2.6	149.5 ± 84.55	0.58	2.7	20–40
12	75 ± 8.7	52 ± 4.2	181.5 ± 57.56	0.57	4.2	20–30
13	71 ± 0.7	56 ± 2.0	144.6 ± 58.51	0.52	9.1	20–50
14	93 ± 1.1	72 ± 1.7	119.3 ± 36.53	0.45	4	60
15	nd	nd	221.2 ± 9.53	0.43	4.2	20–40
16	105 ± 2.4	74 ± 7.7	58.8 ± 1.88	0.60	4.6	15–40
17	86 ± 1.6	45 ± 3.1	159.6 ± 28.04	0.40	2.8	20–40
18	127 ± 2.6	110 ± 10.9	479.6 ± 374.8	0.73	3.6	20–100
19	89 ± 1.7	64 ± 3.2	299.7175.9	0.67	6.2	20–100
20	225 ± 142.5	171 ± 115.1	421 ± 40.41	0.43	nd	20–50
21	nd	nd	126.8 ± 245	nd	2.7	10–50
22	126 ± 4.9	100 ± 9.5	234 ± 29.08	0.50	5.7	20–60

nd not determined.

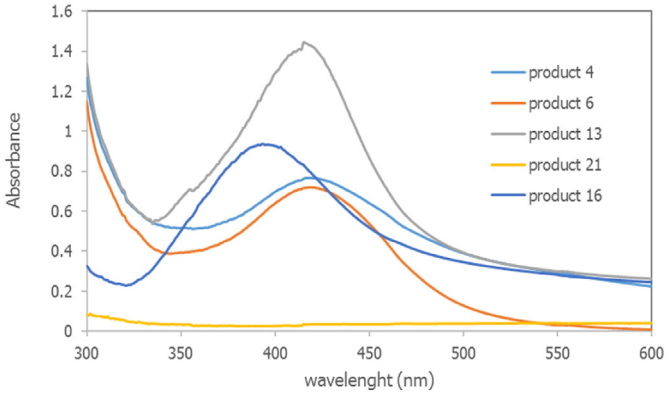

Fig. 2. UV–Vis plasmon resonance signatures. Spectra were recorded for products 4, 6, 13, 16, & 21. Absorbance peaks were observed at 420 nm, 420 nm, 414 nm, 398 nm & no peak, respectively.

protein aggregates or micelle structures (MacCuspie et al., 2011) will inhibit the LSPR effect. It is also possible that colorants may have been added to some of the product suspensions giving a yellow appearance similar to LSPR, but not showing the characteristic absorbance spectra.

3.4. Particle number concentration

Particle number-based concentrations (nanoparticles/mL), in contrast to mass-based concentrations (mg/L) can be useful in several contexts. For example, the European Commission definition of a nanomaterial with respect to product regulation uses the convention of a number-based size distribution (Cascio et al., 2015). Although it has been suggested that no single analytical method is currently available to accomplish the determination of number-based concentration analysis for nanoparticles (in particular AgNPs in consumer products), the combination of methods such as AF4-ICP-MS, CLS, DLS, and TEM has been used toward this goal (Cascio et al., 2015). Our approach for the estimation of number-based concentrations involved the use of NTA with comparisons to CF values and TEM images.

Particle number concentrations for the colloidal silver products were measured using NTA (Fig. 3). Products 4, 6, and 10 showed the largest particle numbers corresponding to the highest total silver concentrations. NTA measurements could not be obtained for products 2, 15, and 21. Reasons for the inability to make these measurements may have included a low total silver concentration in product 2, a high percentage of the very small particles in product 15, and highly aggregated particles in product 21. General limitations for this method also include a measurement concentration window of between 10^8 and 10^9 particles per mL as well as dependencies of the measurement on viscosity, particle refractive index and size limitations for particles less than about 10–20 nm (MacCuspie et al., 2011). Given the uncertainties for the compositions of the product matrices, the presence of very small (<3 nm) silver-containing particles (observed by TEM), and presence of larger particles such as protein aggregates (see Fig. S-4, product 21), the possibility of artifacts for some of the particle number concentration measurement for these suspensions using NTA cannot be ruled out.

3.5. Size determination strategies

Standard polystyrene particles (100, 50, and 40 nm) and well characterized AgNPs (75, 50, 20, 10, and 5 nm) were used to compare hydrodynamic diameter measurements for DLS and NTA against nominal particle sizes from the manufacturer (Table 1). For larger commercial polystyrene standard particles (100, 50, and 40 nm) and AgNPs (75 nm) hydrodynamic diameter values measured by both NTA and DLS were similar to the nominal TEM sizes and similar to the manufacturer reported Z-Avg values (Table 1). For the smaller commercial pvp-stabilized AgNPs (5, 10, 20, and 50 nm), both NTA mean and mode measurements were typically larger than the manufacturer reported nominal size values (Table 1).

For measurement of colloidal silver in consumer products, Z-Avg values ranged from about 55 nm to 484 nm (Table 3). Measurements were made using undiluted suspensions as received except for the most highly concentrated products (4, 6, 10). Polydispersity values ranged from 0.29 to 0.72 with most being >0.5, indicating a high degree of particle size heterogeneity. NTA values for hydrodynamic diameter were significantly smaller than for the DLS measurements with the NTA mode values being typically smaller than the mean measurements for the same product suspension (Table 3). Particle mode diameters were typically under 100 nm with exception of products 18, 20, 22. TEM observations showed very few primary silver particles over 100 nm, suggesting that the larger hydrodynamic diameter values may have been due to particle aggregation, protein aggregates, or micelles some of which may have contained bound AgNP (see Fig. S-4). In addition, several of the NTA particle size measurements could not

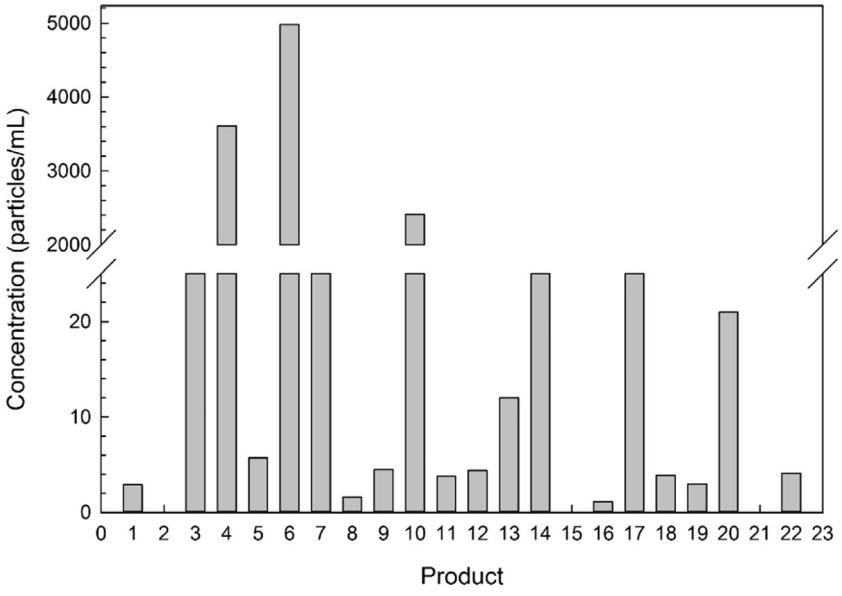

Fig. 3. AgNP Number Concentration. The AgNP number concentrations for colloidal silver products 1–22 were determined using NTA.

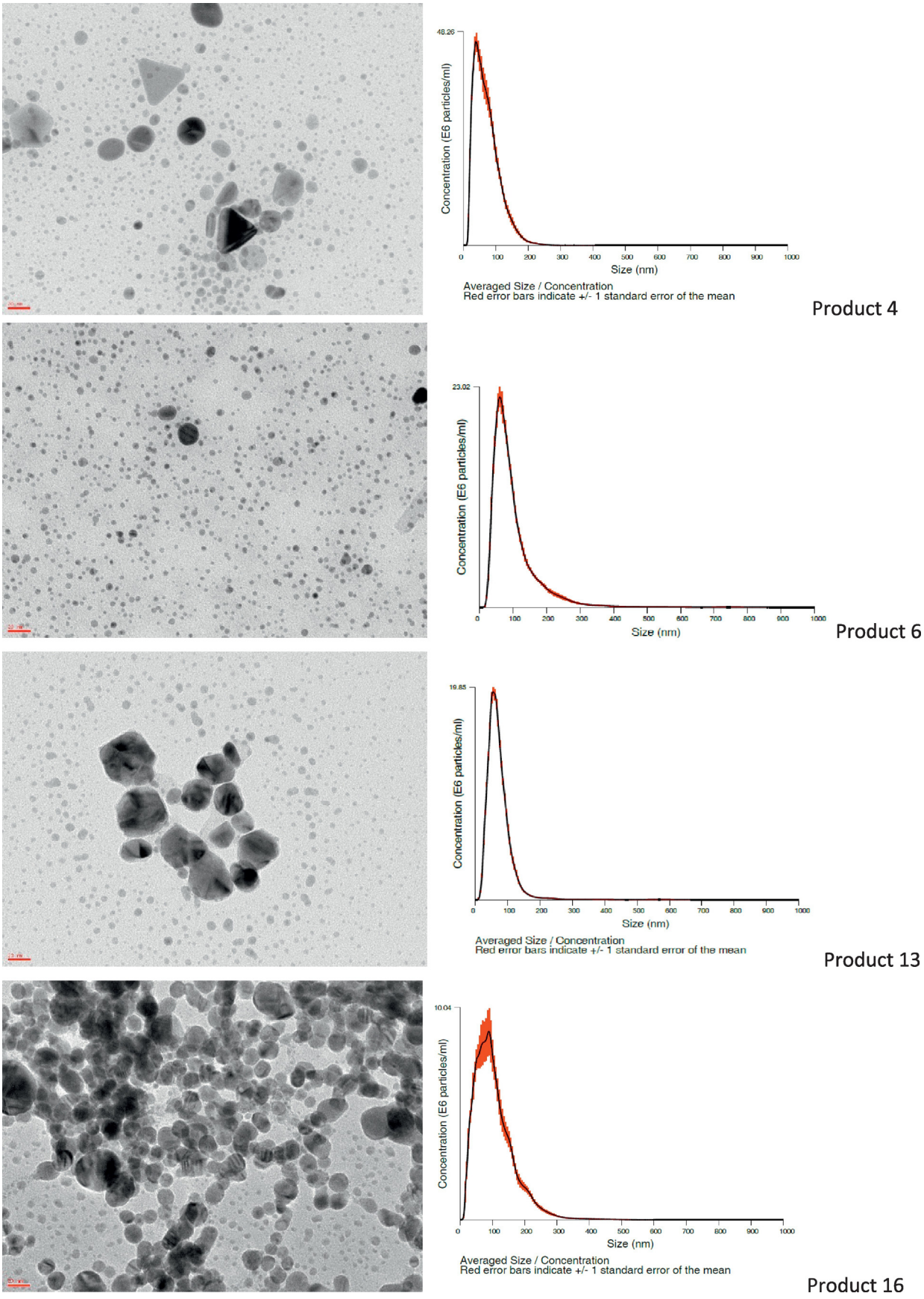

Fig. 4. Representative TEM micrographs and NTA size distributions for products 4, 6, 13 and 16.

be obtained (products 2, 15, and 21) for reasons similar to those discussed in the previous section.

DLS typically shows non-linear variations in scattering intensity that tend to show a bias in the average measurement of larger particles or aggregates. AgNP-hydrodynamic diameter measurements have been reported to be larger than primary particle measurements by TEM (Cascio et al., 2014, 2015). In addition, for both DLS and NTA, the measurements have been shown to be dependent on organic surface coatings and matrix effects, such as viscosity and binding to protein aggregates or micelles, conditions which are likely to be present among the colloidal silver product formulations (Cascio et al., 2014).

3.6. Primary particle size (TEM)

Representative TEM micrographs were obtained for each of the consumer products. For many of the suspensions, the observed particles seemed to fall into one of two categories. These categories included a significantly greater number of very small particles ranging in size from 1 to 10 nm and a smaller population of larger particles ranging from about 20–40 nm (Table 3, Fig. 4, Fig. S-1). The smaller particles were primarily spherical and appeared to be less dense on the micrographs. These small particles are more clearly visible on the micrograph for product 13 (Fig. 4). Although the particles appear to be of lower density, the presence of Ag was confirmed by EDS analysis (Fig. S-2). These smaller particles are similar in size and shape to AgNPs formed using organic reductants, such as green tea leaves and orange peel (Hebbalalu et al., 2013). In product 4, the small particles were also observed by TEM in immediate proximity to and surrounding a larger AgNP (Fig. S-3) similar to those observed as progeny particles formed in situ on SiO_2 TEM grids (Glover et al., 2011), suggesting that in some of the colloidal silver suspensions, AgNPs may be forming in situ in the suspensions and on the TEM grids. Dissolution and in situ formation of smaller AgNPs has been observed in lung tissue (Davidson et al., 2015) and have been described as artifacts during TEM grid preparation (Varenne et al., 2016). For most products, the larger particles were also spherical and showed striations typical of AgNPs (Rogers et al., 2012). Product 4, however, also showed a small population of triangular and pentagonal silver particles (Fig. 4). In addition to micrographs where the silver particles are the primary observed features, suspensions for products 9 and 11 showed the presence of low density squares (possibly organic cubes) with imbedded higher density particles (Fig. S-4). EDS analysis showed the higher density locations to be composed of silver whereas the lower density areas contained little silver but showed the presence of chlorine and sulfur (Fig. S-5). These larger structures appeared to disintegrate under a 1 min. exposure to the electron beam while the imbedded silver spheres remained intact during the same time frame (Fig. S-6). The wide range of particle size, shape and organic structures observed for the AgNPs present in these colloidal silver products would suggest a variety of synthetic methods and formulations were used for these products.

It has been reported that methods used to measure hydrodynamic diameter such as DLS, NTA, and CLS are limited to particles above about 20 nm (Cascio et al., 2014; Varenne et al., 2016). Given the two size ranges of silver-containing particles observed by TEM in these products, as well as the possibility of protein aggregates and micelles, in many of these products, determining the hydrodynamic diameters of the silver-containing products is challenging. Our results also show these limitations reflected by the differences in primary particles size observed by TEM and the average values for hydrodynamic diameter measured using NTA and DLS (Table 3). Nevertheless, in most cases, NTA (particularly mode values) correlated well with the population of larger AgNPs observed by TEM. For about half of the products, the DLS values also appeared to correspond well with the NTA values and the larger particles observed by TEM. In some cases, however, the DLS values may have been biased by larger organic structures (possibly protein aggregates) observed in some of the product suspensions.

3.7. Potential for human exposure

The 22 products investigated for this study claim a diverse array of potential applications ranging from externally applied sanitizing sprays to internally consumed dietary supplements intended to be ingested as a liquid or inhaled from pump sprayers. Consequently, the potential for direct or indirect human exposures is expected to be influenced by a variety of factors. These factors include, the concentration of silver (both soluble and particulate), the suggested dose and frequency of application, adherence to the specified dilution procedure (for concentrated products), and intentional or unintentional misuse of these products.

Toxicological implications for the use of these colloidal silver products not only depend on the form of the silver, but also on the exposure route and dose. Using total silver measurements and recommended dose levels provided on some of the product labels (only 13 of the 18 products indicating internal use, provided recommended dosage levels), estimated Ag doses varied between 5.6 and 961 μg Ag/day (Table S-3). For regular users of AgNP-enabled products, these estimates might be in addition to the 70–90 μg Ag/day exposures estimated to result from the potential use of AgNP-enabled food storage containers. Although these values are lower than the orally administered no observed adverse effects level (NOAEL) for systemic effects (30 mg/kg AgNP) reported by Kim et al. (2010), subtle, but potentially detrimental chronic or long-term effects for lower concentrations of AgNPs have been suggested in the literature. For example, AgNPs were shown to have potentially negative effects on intestinal microvilli (Shahare et al., 2013; Reed et al., 2014). In addition, Van den Brule et al. (2013) suggested that oral exposure of AgNP at human-relevant doses produce significant microbial alterations in the gut. Chronic disruption of the gut microbiome has been associated with numerous adverse physio(patho)logical functions (Aitken and Gewirtz, 2013).

In addition to ingestion exposure, inhalation might also be expected from colloidal silver products equipped with pump spray devices, particularly when the intended use is as a “throat spray”. Although aerosols emitted from these devices produce large liquid droplets that quickly settle onto surfaces (Quadros and Marr, 2010), AgNP distributions within the mouth, throat, nasal cavity, and deeper into the lungs have not been reported for direct inhalation of throat spray Ag colloidal suspensions. Both in vitro and in vivo studies have shown the inflammatory effect of AgNPs on nasal and lung tissue (Jang et al., 2012; Shin and Ye, 2012). In addition, Alessandrini et al. (2017) have shown that AgNPs alter the mouse lung microbiome.

The characterization of physicochemical properties of nanoparticles as supplied in commercially available products is a prerequisite for exposure assessment and risk analysis. One of the properties that is not only fundamental to the definition of nanoparticles but also to their potential function, particularly for AgNPs, is the particle size distribution. Although NTA (mode) measurements showed AgNP hydrodynamic diameters >20 nm and DLS values >50 nm for most products, the number-weighted average particle size by TEM was typically <10 nm and often <5 nm. The presence of these very small particles may have toxicological implications. With respect to potential ecosystem effects, AgNPs <10 nm tend to penetrate cellular membranes to a greater extent than larger AgNPs which may be detrimental to highly sensitive species such as crustaceans as well as other non-targeted species (Ivask et al., 2014). For mammalian systems, smaller AgNPs (<20 nm), typically show a higher degree of cardiovascular toxicity resulting in hemolysis and increased coagulation markers (Gonzalez et al., 2016). This is particularly important for products intended for direct oral ingestion or spray application that may penetrate into lung tissues. This research provided initial AgNP characterization of colloidal silver disinfection products, future studies will explore speciation of soluble and nanoparticulate forms of silver as well as particle transformations at the bio-interface for possible exposures resulting from various use scenarios for these products.

4. Summary

Given the current interest in antimicrobial properties of AgNPs, it is anticipated that the market applications for AgNP-containing products will likely grow in the next decade. In particular, the widespread use of AgNP-enabled spray products shows the potential to result in human exposures through dermal, ingestion and inhalation pathways. Because particle size, shape and surface characteristics have a significant impact on toxicities of AgNPs, a more complete understanding of physiochemical characteristics of the AgNPs present in these consumer products is critical in determining the risks involved with human exposure (Gitipour et al., 2016).

In this study, we report a number of physicochemical characteristics of AgNPs in a broad range of products advertised to contain colloidal silver. Our results demonstrated the presence of silver-containing nanoparticles in all of the selected products advertised to contain colloidal silver. However, a high degree of variability between claimed and measured values for total silver as well as the relative percentage of particulate as compared to soluble silver was noted in many of these colloidal silver products. One significant analytical challenge for characterization of this diverse group of products involved measuring the hydrodynamic diameter values (using DLS and NTA) for the polydisperse population of AgNP including very small (<5 nm) silver-containing particles identified by TEM-EDS. Another analytical challenge involved uncertainties in fractionation due to very small particles as well as the highly variable formulation additives such as “herbs”, amino acids, and/or “essential oils”. It is clear from the presented data that the characterization of AgNPs in these consumer products requires the use of multiple and sometimes redundant methodologies.

Disclaimer

The United States Environmental Protection Agency (U.S. EPA), through its Office of Research and Development (ORD), has funded and managed the research described here. It has been subjected to the Agency's administrative review and has been approved for publication. Certain trade names and company products are mentioned in the text or identified in illustration in order to specify adequately the experimental procedures and equipment used. Such identification does not imply endorsement or recommendation for use by the U.S. EPA. Mention of a specific product or company does not constitute endorsement by the Centers for Disease Control and Prevention. The findings and conclusions in this report are those of the authors and do not necessarily represent the views of the National Institute for Occupational Safety and Health.

Acknowledgements

This project was supported in part by J. Navratilova's appointment to the National Research Council-Research Associateship Program. This project was also supported, in part, by an appointment in the Research Participation Program at the Office of the Research and Development (ORD), EPA administered by the Oak Ridge Institute for Science and Education (92431601) through an interagency agreement between the DOE and EPA. We acknowledge Jennifer Griggs for her technical support in formatting the data for the EPA Science Hub and John Misenheimer for his technical support with the ICP-OES measurements.

Appendix A. Supplementary data

Supplementary data to this article can be found online at https://doi.org/10.1016/j.scitotenv.2017.11.195.

References

Aitken, J.D., Gewirtz, A.T., 2013. Gut microbiota in 2012: toward understanding and manipulating the gut microbiota. Nat. Rev. Gastroenterol. Hepatol. 10, 72–74.
Alessandrini, F., Vennemann, A., Gschwendtner, S., Neumann, A.U., Rothballer, M., Seher, T., Wimmer, M., Kulik, S., Traidl-Hoffmann, C., Schloter, M., Wiemann, M., Schmidt-Weber, C.B., 2017. Pro-inflammatory versus immunomodulatory effects of silver nanoparticles in the lung: the critical role of dose, size and surface modification. Nano 7, 300.
Argentiere, S., Cella, C., Cesaria, M., Milani, P., Lenardi, C., 2016. Silver nanoparticles in complex biological media: assessment of colloidal stability and protein corona formation. J. Nanopart. Res. 18 (8), 253.
Cascio, C., Gilliland, D., Rossi, F., Calzolai, L., Contado, C., 2014. Critical experimental evaluation of key methods to detect, size and quantify Nanoparticulate silver. Anal. Chem. 86 (24), 12143–12151.
Cascio, C., Geiss, O., Franchini, F., Ojea-Jimenez, I., Rossi, F., Gilliland, D., Calzolia, L., 2015. Detection, quantification and derivation of number size distribution of silver nanoparticles in antimicrobial consumer products. J. Anal. Atom. Spectrom. 30 (6), 1255–1265.
Chinnapongse, S.L., MacCuspie, R.I., Hackley, V.A., 2011. Persistence of singly dispersed silver nanoparticles in natural freshwaters, synthetic seawater, and simulated estuarine waters. Sci. Total Environ. 409 (12), 2443–2450.
Davidson, R.A., Anderson, D.S., Van Winkle, L.S., Pinkerton, K.E., Guo, T., 2015. Evolution of silver nanoparticles in the rat lung investigated by X-ray absorption spectroscopy. J. Phys. Chem. 119, 281–289.
Gitipour, A., Thiel, S.W., Scheckel, K.G., Tolaymat, T., 2016. Anaerobic toxicity of cationic silver nanoparticles. Sci. Total Environ. 557, 363–368.
Glover, R.D., Miller, J.M., Hutchinson, J.E., 2011. Generation of metal nanoparticles from silver and copper objects: nanoparticles dynamics on surfaces and potential sources of nanoparticles in the environment. ACSNano 5 (11), 8950–8957.
Gonzalez, C., Rosas-Hernandez, H., Ramirez-Lee, M.A., Salazar-Garcia, S., Ali, S.F., 2016. Role of silver nanoparticles (AgNPs) on the cardiovascular system. Arch. Toxicol. 90, 493–511.
Hagendorfer, H., Kaegi, R., Parlinska, M., Sinnet, B., Ludwig, C., Ulrich, A., 2012. Characterization of silver nanoparticle products using asymmetric flow field flow fractionation with a multidetector approach - a comparison to transmission electron microscopy and batch dynamic light scattering. Anal. Chem. 84 (6), 2678–2685.
Hansen, S.F., Heggelund, L.R., Besora, P.R., Mackevica, A., Boldrin, A., Baun, A., 2016. Nanoproducts - what is actually available to European consumers? Environ. Sci. Nano. 3 (1), 169–180.
Hebbalalu, D., Lalley, J., Nadagouda, M.N., Varma, R.S., 2013. Greener techniques for the synthesis of silver nanoparticles using plant extracts, enzymes, bacteria, biodegradable polymers, and microwaves. ACS Sustain. Chem. Eng. 1, 703–712.
Ivask, A., Juganson, K., Bondarenko, O., Mortimer, M., Aruoja, V., Kasemets, K., Blinova, I., Heinlaan, M., Slaveykova, V., Kahru, A., 2014. Mechanisms of toxic action of Ag, ZnO and CuO nanoparticles to selected ecotoxicological test organisms and mammalian cells in vitro; a comprehensive review. Nanotoxicology 8, 57–71.
Jang, S., Park, J.W., Cha, H.R., Jung, S.Y., Lee, J.E., Jung, S.S., Kim, J.O., Kim, S.Y., Lee, C.S., Park, H.S., 2012. Silver nanoparticles modify VEGF signaling pathway and mucus hypersecretion in allergic airway inlammation. Int. J. Nanomedicine 7, 1329–1343.
Kim, Y.S., Song, M.Y., Park, J.D., Song, K.S., Ryu, H.R., Chung, Y.H., 2010. Subchronic oral toxicity of silver nanoparticles. Part. Fibre Toxicol. 7, 20.
MacCuspie, R.I., Rogers, K., Patra, M., Suo, Z.Y., Allen, A.J., Martin, M.N., Hackley, V.A., 2011. Challenges for physical characterization of silver nanoparticles under pristine and environmentally relevant conditions. J. Environ. Monit. 13 (5), 1212–1226.
Mwilu, S.K., El Badawy, A.M., Bradham, K., Nelson, C., Thomas, D., Scheckel, K.G., et al., 2013. Changes in silver nanoparticles exposed to human synthetic stomach fluid: effects of particle size and surface chemistry. Sci. Total Environ. 447, 90–98.
Quadros, M.E., Marr, L.C., 2010. Environmental and human health risks of aerosolized silver nanoparticles. J. Air Waste Manage. Assoc. 60, 770–781.
Quadros, M.E., Pierson, R., Tulve, N.S., Willis, R., Rogers, K., Thomas, T.A., et al., 2013. Release of silver from nanotechnology-based consumer products for children. Environ. Sci. Technol. 47 (15), 8894–8901.
Ramos, K., Ramos, L., Camara, C., Gomez-Gomez, M.M., 2014. Characterization and quantification of silver nanoparticles in nutraceuticals and beverages by asymmetric flow field flow fractionation coupled with inductively coupled plasma mass spectrometry. J. Chromatogr. A 1371, 227–236.
Reed, R.B., Faust, J.J., Yang, Y., Doudrick, K., Capco, D.G., Hristovski, K., Westerhoff, P., 2014. Characterization of nanomaterials in metal colloid-containing dietary supplement drinks and assessment of their potential interactions after ingestions. ACS Sustain. Chem. Eng. 2 (7), 1616–1624.
Rogers, K.R., Bradham, K., Tolaymat, T., Thomas, D.J., Hartmann, T., Ma, L.Z., et al., 2012. Alterations in physical state of silver nanoparticles exposed to synthetic human stomach fluid. Sci. Total Environ. 420, 334–339.
Sekine, R., Brunetti, G., Donner, E., Khaksar, M., Vasilev, K., Jamting, A.K., Schekel, K.G., Kappen, P., Zhang, H., Lombi, E., 2014. Speciation and lability of Ag-, AgCl-, and Ag2Snanoparticles in soil determined by X-ray absorption spectroscopy and diffusive gradient in thin films. Environ. Sci. Technol. 49, 897–905.
Shahare, B., Yashpal, M., Singh, G., 2013. Toxic effects of repeated oral exposure of silver nanoparticles on small intestine mucosa of mice. Toxicol. Mech. Methods 23 (3), 161–167.
Shin, S.H., Ye, M.K., 2012. The effect of nano-silver on allergic rhinitis model in mice. Clin. Exp. Otorhinolaryngol. 5, 222–227.
Silva, R.M., Anderson, D.S., Peake, J., Edwards, P.C., Patchin, E.S., Guo, T., et al., 2016. Aerosolized silver nanoparticles in the rat lung and pulmonary responses over time. Toxicol. Pathol. 44 (5), 673–686.

Steinhäuser, K.G., Sayre, P., 2017. Reliability of methods and data for regulatory assessments of nanomaterials. Nanoimpact 7, 66–74.
Tolaymat, T., Abdelraheem, W., El Badawy, A., Dionysiou, D., Genaidy, A., 2016. The path towards healthier societies, environments, and economies: a broader perspective for sustainable engineered nanomaterials. Clean Technol. Environ. 18 (7), 2279–2291.
Tulve, N.S., Stefaniac, A.B., Vance, M.E., Rogers, K., Mwilu, S., LeBouf, R.F., Schwegler-Berry, D., Willis, R., Thomas, T.A., Marr, L.C., 2015. Characterization of silver nanoparticles in selected consumer products and its relevance for predicting children's potential exposures. Int. J. Hyg. Environ. Health 218, 345–357.
Van den Brule, S., Ambroise, J., Lecloux, H., Levard, C., Soulas, R., Temmerman, P.-J.D., Palmai-Pallag, M., Marbaix, E., Lison, D., 2013. Dietary silver nanoparticles can disturb microbiota in 2012: toward understanding and manipulating the gut microbiota. Nat. Rev. Gastroenterol. Hepatol. 10, 72–74.
Van Koetsem, F., Verstraete, S., Wallaert, E., Verbeken, K., Van der Meeren, P., Rinklebe, J., et al., 2017. Use of filtration techniques to study environmental fate of engineered metallic nanoparticles: factors affecting filter performance. J. Hazard. Mat. 322, 105–117.
Vance, M.E., Kuiken, T., Vejerano, E.P., McGinnis, S.P., Hochella, M.F., Rejeski, D., et al., 2015. Nanotechnology in the real world: redeveloping the nanomaterial consumer products inventory. Beilstein J. Nanotech. 6, 1769–1780.
Varenne, F., Gaucher-Delmas, M., Violleau, F., Vauthier, C., 2016. Multimodal dispersion of nanoparticles: a comprehensive evolution of size distribution with 9 size measurement methods. Pharm. Res. 33, 1220–1234.
Wasukan, N., Srisung, S., Kulthong, K., Boonrungsiman, S., Maniratanachote, R., 2015. Determination of silver in personal care nanoproducts and effects on dermal exposure. J. Nanopart. Res. 17 (11).

https://www.fda.gov/OHRMS/DOCKETS/98fr/081799a.pdf.
www.epa.gov/pesticide-registration-manual-introduction.